Stripping voltammetry of carbon monoxide oxidation on stepped platinum single-crystal electrodes in alkaline solution

ARTICLE *in* PHYSICAL CHEMISTRY CHEMICAL PHYSICS · AUGUST 2008

Impact Factor: 4.49 · DOI: 10.1039/b803503m · Source: PubMed

2 AUTHORS:

Gonzalo García
Universidad de La Laguna
49 PUBLICATIONS **660** CITATIONS
SEE PROFILE

Marc Koper
Leiden University
302 PUBLICATIONS **9,048** CITATIONS
SEE PROFILE

PCCP
Physical Chemistry Chemical Physics

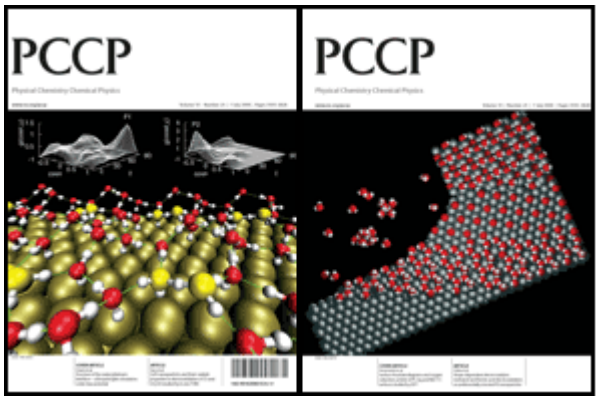

This paper is published as part of a PCCP Themed Issue on:

Electrocatalysis: theory and experiment at the interface

Guest Editor: Andrea Russell

Editorial

Electrocatalysis: theory and experiment at the interface
Phys. Chem. Chem. Phys., 2008
DOI: 10.1039/b808799g

Papers

Structure of the water/platinum interface––a first principles simulation under bias potential
Minoru Otani, Ikutaro Hamada, Osamu Sugino, Yoshitada Morikawa, Yasuharu Okamoto and Tamio Ikeshoji, *Phys. Chem. Chem. Phys.*, 2008
DOI: 10.1039/b803541e

A first-principles study of molecular oxygen dissociation at an electrode surface: a comparison of potential variation and coadsorption effects
Sally A. Wasileski and Michael J. Janik, *Phys. Chem. Chem. Phys.*, 2008
DOI: 10.1039/b803157f

Electrochemical and FTIRS characterisation of NO adlayers on cyanide-modified Pt(111) electrodes: the mechanism of nitric oxide electroreduction on Pt
Angel Cuesta and María Escudero, *Phys. Chem. Chem. Phys.*, 2008
DOI: 10.1039/b717396b

Electrodeposited noble metal particles in polyelectrolyte multilayer matrix as electrocatalyst for oxygen reduction studied using SECM
Yan Shen, Markus Träuble and Gunther Wittstock, *Phys. Chem. Chem. Phys.*, 2008
DOI: 10.1039/b802688b

CoPt nanoparticles and their catalytic properties in electrooxidation of CO and CH_3OH studied by *in situ* FTIRS
Qing-Song Chen, Shi-Gang Sun, Zhi-You Zhou, Yan-Xin Chen and Shi-Bin Deng, *Phys. Chem. Chem. Phys.*, 2008
DOI: 10.1039/b802047g

Kinetic studies of adsorbed CO electrochemical oxidation on Pt(335) at full and sub-saturation coverages
Prachak Inkaew and Carol Korzeniewski, *Phys. Chem. Chem. Phys.*, 2008
DOI: 10.1039/b804507k

Formic acid electrooxidation on Pd in acidic solutions studied by surface-enhanced infrared absorption spectroscopy
Hiroto Miyake, Tatsuhiro Okada, Gabor Samjeské and Masatoshi Osawa, *Phys. Chem. Chem. Phys.*, 2008
DOI: 10.1039/b805955a

Voltammetric surface dealloying of Pt bimetallic nanoparticles: an experimental and DFT computational analysis
Peter Strasser, Shirlaine Koh and Jeff Greeley, *Phys. Chem. Chem. Phys.*, 2008
DOI: 10.1039/b803717e

Unique activity of Pd monomers: hydrogen evolution at AuPd(111) surface alloys
Y. Pluntke, L. A. Kibler and D. M. Kolb, *Phys. Chem. Chem. Phys.*, 2008
DOI: 10.1039/b802915f

Shape-dependent electrocatalysis: methanol and formic acid electrooxidation on preferentially oriented Pt nanoparticles
J. Solla-Gullón, F. J. Vidal-Iglesias, A. López-Cudero, E. Garnier, J. M. Feliu and A. Aldaz, *Phys. Chem. Chem. Phys.*, 2008
DOI: 10.1039/b802703j

The role of adsorbed hydroxyl species in the electrocatalytic carbon monoxide oxidation reaction on platinum
Anthony R. Kucernak and Gregory J. Offer, *Phys. Chem. Chem. Phys.*, 2008
DOI: 10.1039/b802816h

An unexpected enhancement in methanol electro-oxidation on an ensemble of Pt(111) nanofacets: a case of nanoscale single crystal ensemble electrocatalysis
Ceren Susut, George B. Chapman, Gabor Samjeské, Masatoshi Osawa and YuYe Tong, *Phys. Chem. Chem. Phys.*, 2008
DOI: 10.1039/b802708k

Surface Pourbaix diagrams and oxygen reduction activity of Pt, Ag and Ni(111) surfaces studied by DFT
Heine A. Hansen, Jan Rossmeisl and Jens K. Nørskov, *Phys. Chem. Chem. Phys.*, 2008
DOI: 10.1039/b803956a

Electrocatalytic mechanism and kinetics of SOMs oxidation on ordered PtPb and PtBi intermetallic compounds: DEMS and FTIRS study
Hongsen Wang, Laif Alden, F. J. DiSalvo and Héctor D. Abruña, *Phys. Chem. Chem. Phys.*, 2008
DOI: 10.1039/b801473f

Combinatorial screening of PtTiMe ternary alloys for oxygen electroreduction
Ting He and Eric Kreidler, *Phys. Chem. Chem. Phys.*, 2008
DOI: 10.1039/b802818b

Electrochemical study on the adsorption of carbon oxides and oxidation of their adsorption products on platinum group metals and alloys
Hanna Siwek, Mariusz Lukaszewski and Andrzej Czerwinski, *Phys. Chem. Chem. Phys.*, 2008
DOI: 10.1039/b718286b

Ethanol electrooxidation onto stepped surfaces modified by Ru deposition: electrochemical and spectroscopic studies
V. Del Colle, A. Berná, G. Tremiliosi-Filho, E. Herrero and J. M. Feliu, *Phys. Chem. Chem. Phys.*, 2008
DOI: 10.1039/b802683a

The effects of the specific adsorption of anion on the reactivity of the Ru(0001) surface towards CO adsorption and oxidation: *in situ* FTIRS studies
J. M. Jin, W. F. Lin and P. A. Christensen, *Phys. Chem. Chem. Phys.*, 2008
DOI: 10.1039/b802701c

Experimental and numerical model study of the limiting current in a channel flow cell with a circular electrode
J. Fuhrmann, H. Zhao, E. Holzbecher, H. Langmach, M. Chojak, R. Halseid, Z. Jusys and J. Behm, *Phys. Chem. Chem. Phys.*, 2008
DOI: 10.1039/b802812p

Using layer-by-layer assembly of polyaniline fibers in the fast preparation of high performance fuel cell nanostructured membrane electrodes
Marc Michel, Frank Ettingshausen, Frieder Scheiba, André Wolz and Christina Roth, *Phys. Chem. Chem. Phys.*, 2008
DOI: 10.1039/b802813n

Stripping voltammetry of carbon monoxide oxidation on stepped platinum single-crystal electrodes in alkaline solution
Gonzalo García and Marc T. M. Koper, *Phys. Chem. Chem. Phys.*, 2008
DOI: 10.1039/b803503m

Pt_xRu_{1-x}/Ru(0001) surface alloys—formation and atom distribution
H. E. Hoster, A. Bergbreiter, P. M. Erne, T. Hager, H. Rauscher and R. J. Behm, *Phys. Chem. Chem. Phys.*, 2008
DOI: 10.1039/b802169d

Stripping voltammetry of carbon monoxide oxidation on stepped platinum single-crystal electrodes in alkaline solution

Gonzalo García and Marc T. M. Koper*

Received 28th February 2008, Accepted 15th April 2008
First published as an Advance Article on the web 23rd May 2008
DOI: 10.1039/b803503m

The electrochemical oxidation of a CO adlayer on Pt[n(111)×(111)] electrodes, with n = 30, 10, and 5, Pt(111), Pt(110) as well as a Pt(553) electrode (with steps of (100) orientation) in alkaline solution (0.1 M NaOH) has been studied using stripping voltammetry. On these electrodes, it is possible to distinguish CO oxidation at four different active oxidation sites on the surface, *i.e.* sites with (111), (110) and (100) orientation, and kink sites. The least active site for CO oxidation is the (111) terrace site. Steps sites are more active than the (111) terrace sites, the (110) site oxidizing CO at lower potential than the (100) site. The CO oxidation feature with the lowest overpotential (oxidation potential as low as 0.35 V *vs.* RHE) was ascribed to oxidation of CO at kink sites. The amount of CO oxidized at the active step or kink sites *vs.* the amount of CO oxidized at the (111) terrace sites depends on the concentration of the active sites and the time given for the terrace-bound CO to reach the active site. By performing CO stripping on the stepped surfaces at different scan rates, the role of CO surface diffusion is probed. The possible role of electronic effects in explaining the unusual activity and dynamics of CO adlayer oxidation in alkaline solution is discussed.

1. Introduction

The oxidation of carbon monoxide on a platinum electrode is an important model reaction and practical reaction in fuel cell catalysis.[1] It is well known that the kinetics of CO oxidation on platinum does not only depend on the structure of the platinum surface,[2–6] but also on the properties of the electrolyte solution.[7–9] Interestingly, alkaline electrolytes exhibit the lowest overpotential for CO oxidation on platinum,[7–9] even on the relative reversible hydrogen electrode (RHE) scale, which is supposed to correct for "trivial" pH effects. Systematic studies of the mechanism on CO oxidation on well-defined platinum surfaces in alkaline solution have been less forthcoming, as no good alkaline electrolytes for practical utilization in real low-temperature fuel cells have as yet been developed, in addition to the problem of carbonate formation in alkaline media. However, as new alkaline electrolytes are being introduced and tested,[10] and new concepts such as electrolyte circulation are being suggested,[11] one may expect a revival of interest in fuel cell catalysis in alkaline media, especially because, from the catalytic point-of-view, they seem to exhibit activities that for many relevant reactions are significantly higher than those observed in acidic media.[12]

In spite of the fact that there is consensus in the literature about the higher relative catalytic activity for CO oxidation on platinum in alkaline solution compared to acidic solution, there is little molecular-level understanding as to why this is. Markovic *et al.*[1,7] and, more recently, Spendelow and Wieckowski and co-workers,[8,9] have studied CO oxidation on Pt(111) in alkaline solution, and indeed observed that the CO oxidation potential can be more than 200 mV lower than in perchloric acid solution (for which the influence of anion adsorption can be neglected), both for continuous CO oxidation and for CO stripping. Both groups have ascribed the enhanced oxidation characteristics of CO in alkaline media to a higher affinity of OH for the platinum surface, especially for the step and defect sites. In our opinion, however, this explanation must be incomplete, as all the "trivial" pH effects must have been accounted for by referring the electrode potential to the RHE scale. In other words, the respective reactions for OH_{ads} formation in acidic and alkaline solution:

$$H_2O \leftrightarrow OH_{ads} + H^+ + e^- \quad (1)$$

$$OH^- \leftrightarrow OH_{ads} + e^- \quad (2)$$

should take place at the same potential on the RHE scale if the adsorption strength of OH_{ads} to the platinum adsorption site is the same in both media. Indeed, the potential region of OH adsorption on the Pt(111) terrace is at essentially the same potentials (on the RHE scale) for both acidic and alkaline media (see Fig. 1), although the voltammetric peaks in both media are not exactly the same and the final OH coverage on the Pt(111) surface seems to be higher in alkaline media than in acidic media. However, these different coverages have not been invoked in explaining the enhanced activity in alkaline media. Close inspection of Fig. 1 would even suggest that OH adsorption on the Pt(111) terrace starts at a lower potential in acidic solution than in alkaline solution, rather than the reverse. It is not clear how on defects this situation would be drastically different, as suggested implicitly by Markovic *et al.*[7] and Spendelow *et al.*[9] We conclude that simply referring to a higher affinity of OH for Pt in alkaline solution compared to acidic solution, is an unsatisfactory and incomplete

Leiden Institute of Chemistry, Leiden University, PO Box 9502, RA Leiden, 2300, The Netherlands. E-mail: m.koper@chem.leidenuniv.nl

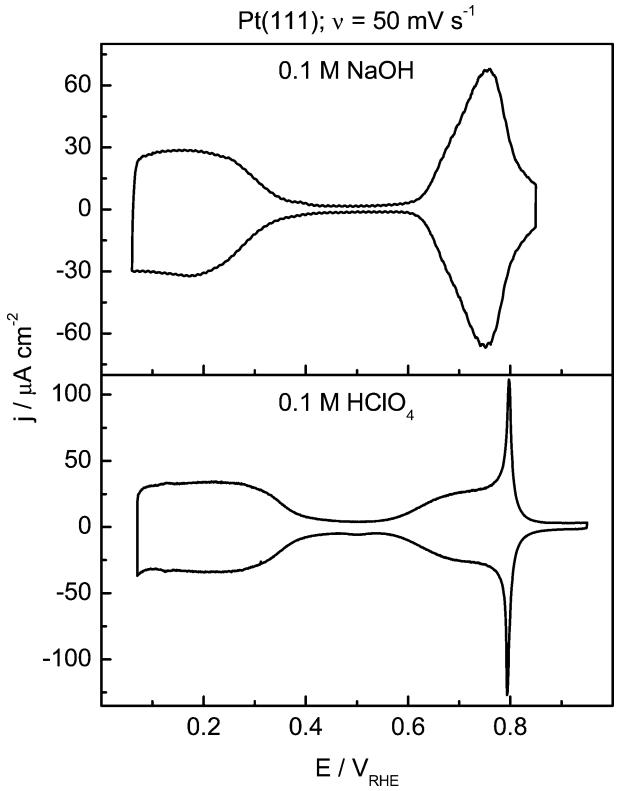

Fig. 1 Cyclic voltammograms of Pt(111) in 0.1 M $HClO_4$ and 0.1 M NaOH, sweep rate 50 mV s^{-1}.

explanation, and there must be a more non-trivial property of alkaline media, or rather of the Pt/alkaline solution interface, that makes it so reactive towards CO oxidation.

In acidic media, it is now well-established that step and defect sites possess a unique activity for CO oxidation, even to the extent that on a series of stepped Pt electrodes, it has been concluded that all CO, both those initially adsorbed at or near the step and those initially adsorbed on the terrace, react to CO_2 at the step sites.[5,6] CO oxidation on the Pt(111) terrace is essentially negligible, and all CO will diffuse rapidly to the step or defect sites and get oxidized there. Spendelow *et al.*[9] recently came to a similar conclusion for CO oxidation on well-ordered and disordered Pt(111) in aqueous NaOH solutions. On the basis of their experiments with slightly disordered Pt(111) electrodes, they claimed that defect-bound OH is active for Langmuir-Hinshelwood CO oxidation at low potential. Nevertheless, since CO stripping in their experiments was always characterized by two peaks, a low-potential "pre-peak" and a high-potential "main peak", the main peak corresponding to CO oxidation from terraces, Spendelow *et al.*[9] also concluded at low CO coverage, CO is apparently unable to react with defect-bound OH. This situation is sufficiently different from acidic solution that it prompted us to investigate the influence of defects on CO oxidation on Pt electrodes in alkaline solution more systematically by employing a series of stepped single-crystal Pt electrodes. This paper is a first in a series of papers on the mechanism of CO oxidation on Pt in alkaline solution, in which we give a detailed report of the stripping voltammetry of chemisorbed CO on single-crystalline Pt electrodes. Chronoamperometry and *in situ* spectroscopy will be reported in future work. Our stripping voltammetry results significantly extend the previous work of Spendelow and Wieckowski *et al.*,[9] and are sufficiently different from similar previous experiments in acidic media, to warrant a separate paper. Most importantly, we will show that in alkaline solution, slow CO surface diffusion on terraces appears to play a surprisingly crucial role, in strong contrast to acidic media. This conclusion once more attests to the fundamentally different catalytic properties of platinum in alkaline media as compared to acidic media, which we believe remain to be fully understood.

2. Experimental

Bead-type single-crystals of Pt[n(111)×(111) (or equivalently Pt[(n − 1) (111)×(110)]) orientation—Pt(553) with n = 5, Pt(554) n = 10, Pt(151514) n = 30, Pt(111) and Pt(110), as well as a Pt(533) electrode (with steps of (100) orientation separated by 5 atom wide (111) terraces), prepared according to the Clavilier method,[13] were used in this study. Before each experiment the single-crystal electrode was flame annealed and cooled down to room temperature in a H_2 + Ar atmosphere, after which it was transferred to the cell under the protection of a droplet of deoxygenated water.

A platinum wire was used as a counter electrode and a reversible hydrogen electrode (RHE) in the supporting electrolyte was employed as the reference electrode. All potentials in the text are referred to this electrode. Electrochemical measurements were performed with a computer-controlled Autolab PGSTAT12 potentiostat-galvanostat. All experiments were carried out in an electrochemical cell using a three-electrode assembly at room temperature. The cell and all glassware were cleaned by boiling in a mixture of 1 : 1 concentrated nitric and sulfuric acid, followed by washing with ultra-pure water.

Experiments were carried out in 0.1 M NaOH, prepared from high purity reagents (99,99%, Merck, "Suprapur") and ultra-pure water (Millipore MilliQ gradient A10 system, 18.2 MΩ cm, 2ppb total organic carbon). Argon (N66) was used to deoxygenate all solutions and CO (N47) to dose CO. CO stripping voltammograms were obtained after bubbling CO through the cell for 3 min while keeping the Pt electrode in the bulk of the solution at 0.10 V, followed by argon purging for 15 min to remove the excess CO. Finally, the working electrode was brought back into the meniscus configuration and the oxidation of the CO adlayer was initiated by scanning the potential in the positive direction.

3. Results and discussion

Blank voltammetry

In their studies of CO oxidation on Pt(111) in alkaline solution, Spendelow *et al.*[9] observed that repeated cycling of the electrode, both in the absence and presence of CO on the electrode surface, leads to a mild surface disordering that can be detected in both the blank voltammetry and by *in situ* scanning tunneling microscopy (STM) images. Specifically,

cycling the potential up to 1.25 V (*vs.* RHE) results in the formation of small Pt islands with a diameter between 1–4 nm as observed by STM. In the blank voltammetry, these islands give rise to additional small peaks at 0.27 V (corresponding to (110) step sites), 0.40 V (corresponding to (100) step sites) and 0.49 V (corresponding to kink sites), according to Spendelow *et al*. We have observed similar effects during CO stripping on stepped Pt electrodes. Since these low-coordination sites have a significant impact of the oxidation kinetics of surface-bonded CO, it is important to briefly discuss the influence of positive potential excursions, particularly in the presence of CO on the surface, on the structure of the stepped Pt electrodes used in this study.

We will limit ourselves to the information that can be extracted from changes in the blank voltammetric profile before CO stripping (''well-ordered'' surface) and after CO stripping (slightly ''disordered'' surface). Fig. 2 shows these curves for the six surfaces under consideration here, *i.e*. Pt(111), Pt(15 15 14), Pt(554), Pt(553), Pt(533) and Pt(110). These blank voltammetric profiles agree well with previous literature results.[14] For Pt(111) and the stepped surfaces, the effects of CO stripping on blank voltammetry are relatively minor. For the Pt(554) and Pt(553) surfaces, we see the development of a small feature at 0.40 V after CO stripping, which may be ascribed to step-like sites of (100) orientation (by comparison to the blank voltammetry for Pt(533) in Fig. 2). Similar observations were made by Spendelow *et al*.,[9] after potential excursions to >1.2 V (*vs.* RHE). We did not observe the development of a feature at *ca*. 0.49 V, which Spendelow observed after surface oxidation of their Pt(111) electrode and which they ascribed to kink sites belonging to small Pt surface islands observed in STM, as we never submitted our electrodes to these ''extreme'' conditions. We believe that the voltammograms shown in Fig. 2 suggest that changes in the surface structure of Pt(111) and the stepped electrodes are small, albeit not completely absent. This gives us confidence that the CO stripping features to be discussed in the next paragraphs can be related meaningfully to the nominal crystallographic plane, and the effect of potential- or reaction-induced disordering should be minimal. On the other hand, larger differences between the blank voltammetry before and after CO stripping were observed for the Pt(110) electrode. Given the lower stability of the more open (110) surface, this is not so surprising. Therefore, for the Pt(110) electrode we cannot exclude the effect of potential- and/or reaction-induced disordering.

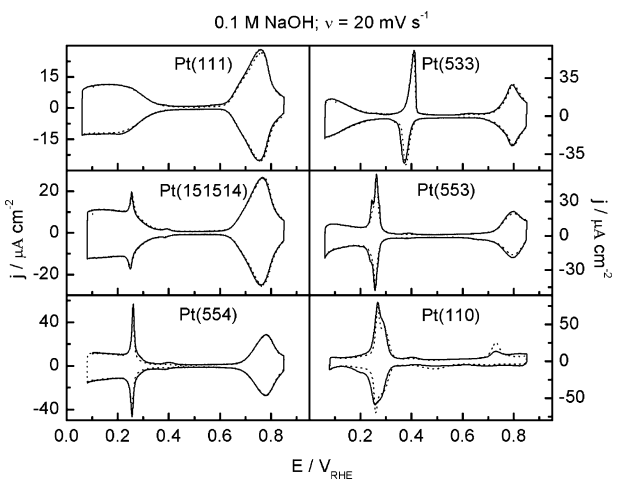

Fig. 2 Cyclic voltammograms before (dotted line) and after (solid line) CO stripping of Pt(111), Pt(151514), Pt(554), Pt(533), Pt(553) and Pt(110) in 0.1 M NaOH, sweep rate 20 mV s^{-1}.

CO stripping—comparing the CO stripping profiles on the six Pt electrodes

Fig. 3 compares the stripping voltammetry observed for a CO saturated Pt electrode for the six different Pt surfaces considered in this study at a scan rate of 20 mV s^{-1}. In agreement with the results published by Spendelow *et al*., the stripping peak on Pt(111) consists of two features: a small ''prepeak'' or ''prewave'' (0.4–0.7 V) that Spendelow *et al*.[9] attributed to oxidation of CO at defect sites, and a main peak (0.7–0.8 V) corresponding to CO oxidation at the Pt(111) terrace sites. As mentioned in the Introduction, Spendelow *et al*. reached their conclusion on the basis of comparing CO stripping on well-ordered and disordered Pt(111). A more direct way of assessing the role of step or defect sites, is to compare the CO stripping voltammogram on a series of stepped Pt electrodes, as in Fig. 3.

First of all, it is clearly seen that the ''terrace'' peak between 0.7 and 0.8 V decreases as the step density increases, but remains essentially in the same potential region. On Pt(15 15 14) the peak is still significant, on Pt(554) it is rather small, on Pt(553) it has almost disappeared, whereas on Pt(110) there is no such peak. Secondly, on the stepped surfaces Pt(15 15 14), Pt(554) and Pt(553) the ''prewave'' region exhibits two or even three different features. The prewave starts at *ca*. 0.35 V, leading to a peak or a plateau at *ca*. 0.45 V. A large sharp peak is then observed at 0.62 V [Pt(15 15 14)], 0.61 V [Pt(554)] and 0.59 V [Pt(553)]. Finally, a small sharp feature is visible at 0.7 V on the Pt(554), Pt(553), and also on the Pt(110) electrode. To start with the latter feature, we believe it is due to CO oxidation on a small number or (100)-type step sites, as

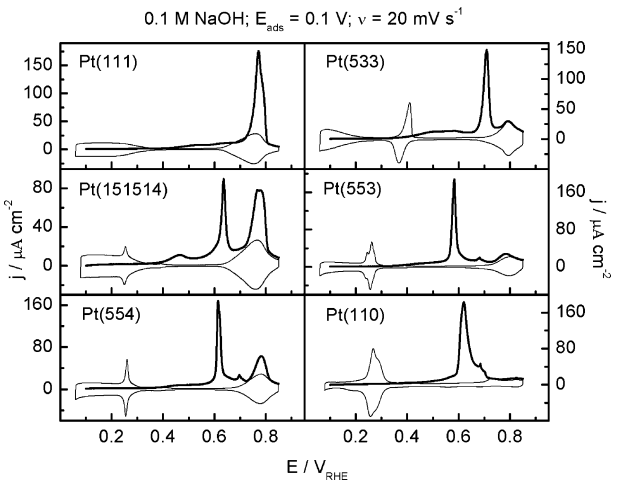

Fig. 3 CO stripping (thick solid line) and the subsequent cyclic voltammogram (thin solid line) for Pt(111), Pt(151514), Pt(554), Pt(533), Pt(553) and Pt(110) in 0.1 M NaOH, sweep rate 20 mV s^{-1}, E_{ads} = 0.1 V.

the step-related peak on a Pt(533) electrode, *i.e.* a surface with (111)-type terraces and (100) steps, occurs at exactly the same potential (see the corresponding CO stripping profile on Pt(533) in Fig. 3). Also, CO stripping on a Pt(100) electrode in alkaline solution shows a peak at this potential (results not shown). The large peak at *ca.* 0.60 V is attributed to CO oxidation at the (110) step sites. Finally, it is tempting to tentatively ascribe the current at potentials lower than 0.5 V to CO oxidation at low-coordinated "kink"-type sites, following the suggestion made by Spendelow *et al.*[9] These authors observed a substantially enhanced oxidation of CO in the prewave region between 0.4 and 0.6 V on a Pt(111) electrode that was lightly disordered such that it showed a blank voltammetric peak at 0.49 V.

The CO oxidation stripping voltammetry on stepped Pt electrodes in alkaline solutions is remarkably different from that in acidic solutions.[4] The results described above strongly suggest that all the different Pt surface sites lead to different distinguishable peaks in the CO stripping voltammetry. In acidic solutions, the stripping of a saturated CO monolayer on stepped Pt electrodes leads typically to only a single main peak, corresponding to CO oxidation at the step sites. Multiple stripping peaks may be observed for subsaturated CO layers, but without a clear one-to-one correspondence to the density of certain Pt surface-site ensembles.[4] A prewave or prepeak may also be observed in CO stripping from a Pt(111) electrode in acidic solution, especially if the CO was adsorbed in the hydrogen region.[1,15] The prewave has also been described to CO oxidation at certain defect sites, though not necessarily kink sites.[1] In any case, the remarkable conclusion from Fig. 3 is that in alkaline solution, the CO oxidation stripping profile can apparently be deconvolved into the contributions from the various Pt sites which have a different activity towards CO oxidation. Such a deconvolution would only be possible if the mobility of CO adsorbed on the terraces (the sites with the highest oxidation overpotential) is low. A high mobility would imply that CO would diffuse to the site with the lowest overpotential to get oxidized there, as is observed on stepped Pt electrodes in acidic media. To investigate the effect of a possibly low CO surface mobility on the terraces, we have measured the stripping voltammetry at different scan rates.

Pt(111)

Fig. 4 shows the CO stripping voltammetry on Pt(111) at different scan rates between 5 and 500 mV s^{-1}. It is clearly observed from this Figure that the prewave is more prominent at lower scan rates, which suggests that at a lower scan rate CO has more time to reach the active oxidation sites. Fig. 5 plots the potential of the prepeak and the main peak as a function of the logarithm of the scan rate. At higher scan rates, it was not possible to determine an accurate position of the prewave. The slope of these curves should in principle give the Tafel slope,[16] but we believe that in this particular case the interpretation of the slope is not that straightforward, as explained in the next section. Nevertheless, these slopes agree reasonably well with the slopes given by Spendelow *et al.*[9] (though they obtained the Tafel slopes in a different way).

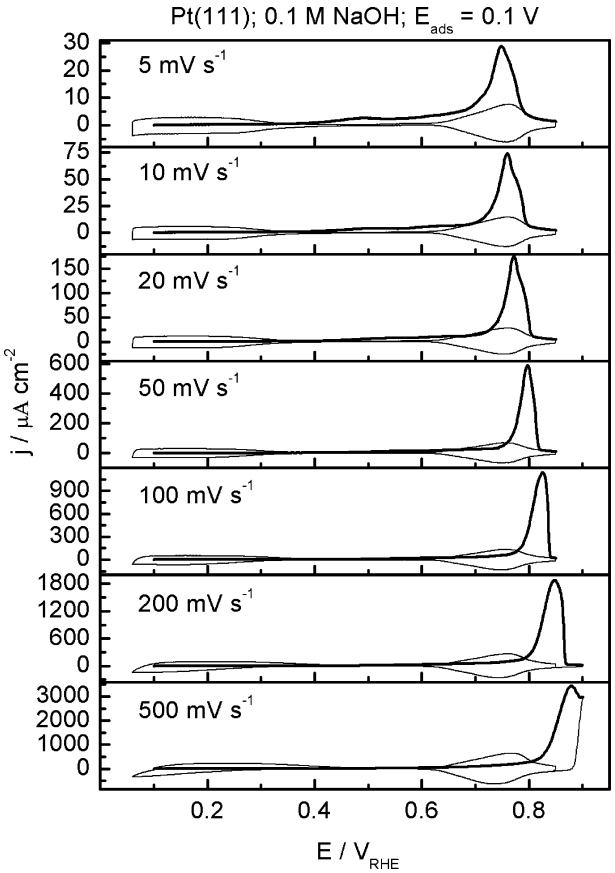

Fig. 4 CO stripping (thick solid line) and the subsequent cyclic voltammogram (thin solid line) for Pt(111) in 0.1 M NaOH at different sweep rates, E_{ads} = 0.1 V.

They reported a Tafel slope of 130 mV dec^{-1} for the prepeak, compared to 118 mV dec^{-1} obtained by our method, and of 73 mV dec^{-1} for the main peak, compared to 67 mV dec^{-1} acquired by our procedure.

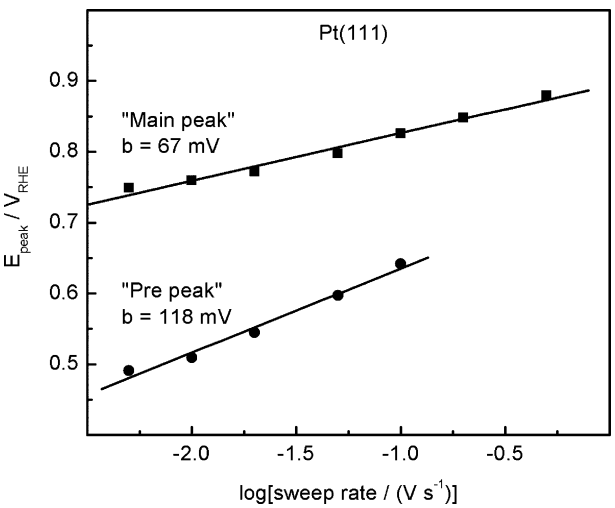

Fig. 5 Peak potential for CO oxidation *versus* the logarithm of the sweep rate for Pt(111). Solid lines are the least-squares fits of the data.

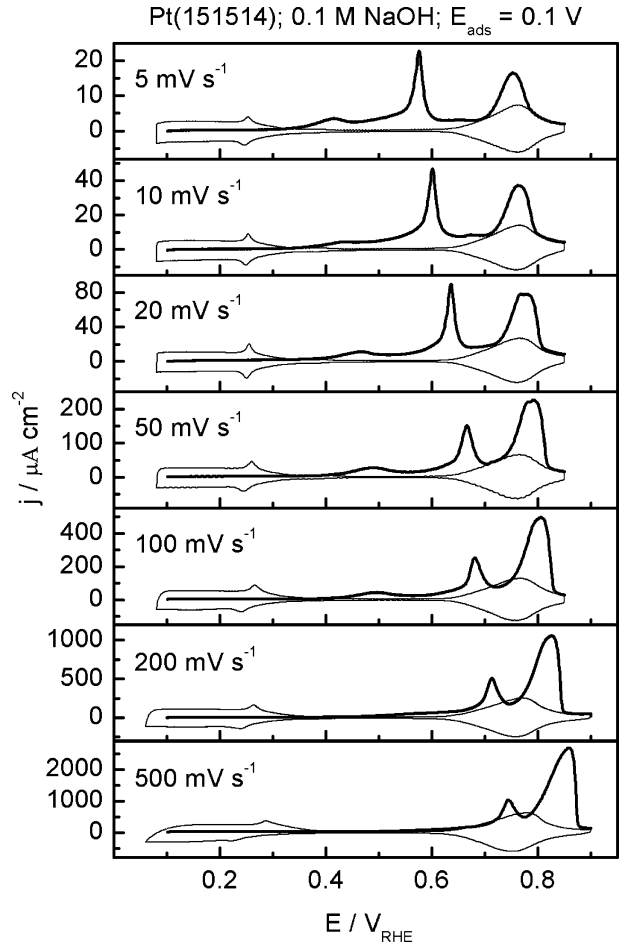

Fig. 6 CO stripping (thick solid line) and the subsequent cyclic voltammogram (thin solid line) for Pt(151514) in 0.1 M NaOH at different sweep rates, E_{ads} = 0.1 V.

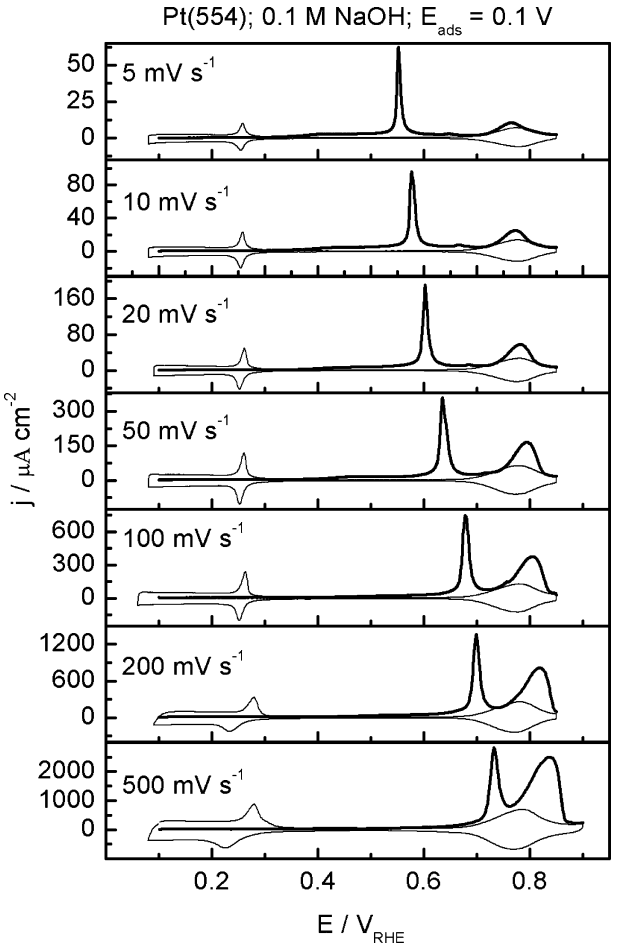

Fig. 7 CO stripping (thick solid line) and the subsequent cyclic voltammogram (thin solid line) for Pt(554) in 0.1 M NaOH at different sweep rates, E_{ads} = 0.1 V.

Pt(15 15 14), Pt(554) and Pt(553)

Fig. 6–8 show the CO stripping voltammetry on the stepped surfaces Pt(15 15 14), Pt(554) and Pt(553) at different scan rates between 5 and 500 mV s^{-1}. On these electrodes, the effect of the scan rate on the amount of CO oxidized in the steps and on the terraces is very conspicuous. On Pt(15 15 14), at high scan rate (500 mV s^{-1}), only a small amount of CO is oxidized in a prepeak at *ca.* 0.75 V, whereas at low scan rate (5 mV s^{-1}) more than half of the CO is oxidized in the prewave (peak at 0.58 V). On the Pt(554) and Pt(553) electrodes, for the highest scan rate a significant amount of CO is oxidized at the terrace sites, whereas for the lowest scan rate (5 mV s^{-1}), practically all CO is oxidized at the step sites and only a small amount of CO is oxidized on the terrace. This latter observation is in contrast to the results obtained for Pt(111) by Spendelow *et al.*,[9] who claimed that at a CO coverage below 0.2 monolayer, CO is too strongly bound to the terrace to react with defect-bound OH. Apparently, this statement needs refinement. The real amount of CO that is able to react with defect- or step-bound OH depends on the step density and the time that the terrace-bound CO is given to reach these active sites, as can be seen in Fig. 9, in which the charge corresponding to CO oxidation on the terrace (Q_{ter}) is plotted *versus* the step density (θ_{step}). Q_{ter} was determined by integration of the CO stripping current of the corresponding voltammetric peak, subtracted by the integrated current in the blank voltammetry in the same potential window. Fig. 9 shows the change of Q_{ter} with the scan rate for each stepped surface, suggesting a slow CO diffusion on the terraces. Only at the higher scan rates is it possible to observe a linear relationship between Q_{ter} and the step density (the nonlinearity for the highest scan rate 500 mV s^{-1} is probably due to the difficulty in accurately estimating Q_{ter}). At high scan rate, CO diffusion on the terrace is negligible and because of this the charge corresponding to the CO stripping in this feature correlates well with the step and terrace density.

In order to check in a more quantitative way that the effect of the scan rate on the voltammetry shown in Fig. 6–8 is due to a finite mobility of CO on the (111) terrace, we need to perform some kind of Cottrell analysis. To this end, we analyze the amount of CO oxidized on the terrace (Q_{ter}) or the amount of CO oxidized at the (110) steps (Q_{step}) as a function of the scan rate. The total oxidation charge is a sum of these two contributions and a "rest" contribution corresponding to oxidation at the low-coordination "kink" sites and the small number of (100) steps, $Q_{tot} = Q_{step} + Q_{ter} + Q_{rest}$,

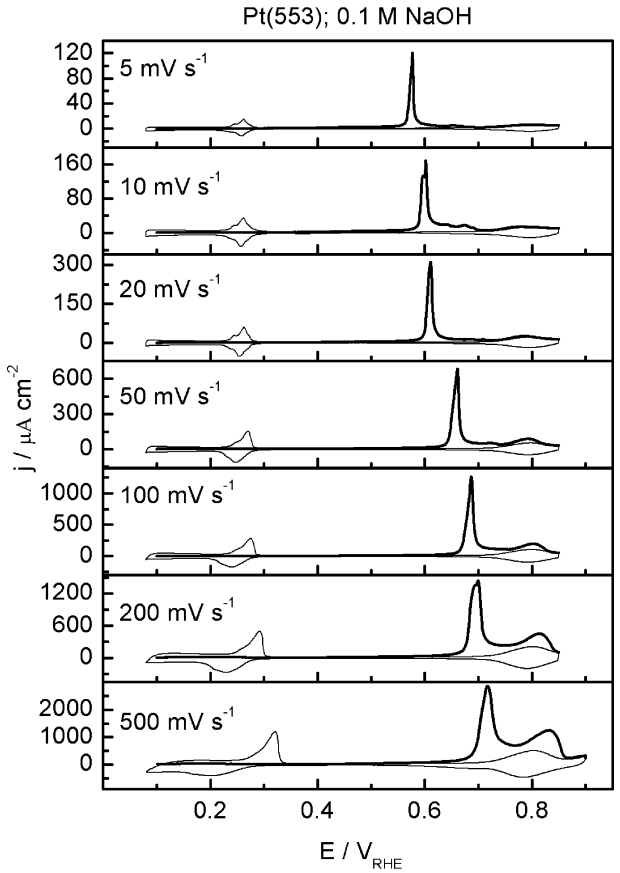

Fig. 8 CO stripping (thick solid line) and the subsequent cyclic voltammogram (thin solid line) for Pt(553) in 0.1 M NaOH at different sweep rates, E_{ads} = 0.1 V.

which should be a constant for each surface. If communication between steps and terraces is accommodated by diffusion, then Q_{step} and Q_{ter} should depend linearly on the square root of the scan rate, $v^{1/2}$, by analogy with the usual scaling laws for diffusion-limited processes.[17] This scaling law is confirmed for the Pt(554) and the Pt(553) surface, as can be seen in Fig. 10. However, Q_{ter} or Q_{step} *vs.* $v^{1/2}$ does not give a straight line for the Pt(15 15 14) surface (see also Fig. 10). In fact, we find that for this surface, Q_{ter} *vs.* ln(v) seems to follow a linear relationship, the exact physical meaning and significance of which is unclear. Most likely, the deviation at lower scan rates for this surface is due to the higher number of kink sites on this surface (as is visible from the voltammetry in Fig. 2 and 6) leading to relatively more CO being oxidized at kink sites on this surface for the lower scan rates. Clearly, a full understanding of these trends requires detailed kinetic modeling, as well as transient measurements.

Fig. 11 shows the results of another CO stripping experiment on the Pt(15 15 14), Pt(554) and Pt(553) electrodes. In this experiment, the scan is reversed after the first prepeak on Pt(15 15 14) and Pt(554), see the solid lines in Fig. 11. In the following scan through the hydrogen region it is observed that the electrodes are still largely blocked by the adsorbed CO. In the next CO stripping scan and the first scan for the Pt(553) electrode, the scan direction is reversed after the second prepeak, corresponding to the oxidation of CO at the (110)

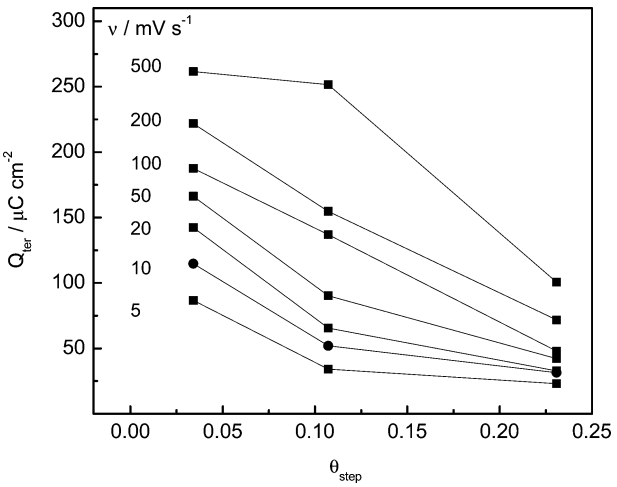

Fig. 9 Charge densities corresponding to CO oxidation on the (111) terrace, Q_{ter}, *versus* step density for Pt(151514), Pt(554), Pt(553) at different sweep rates.

step sites (dashed lines). Interestingly, in the subsequent scan through the hydrogen region, hydrogen adsorption onto the terrace is now visible, but the peak corresponding to hydrogen adsorption on the (110) steps is still blocked for the surfaces with lower step density, while for the Pt(553) electrode, both terrace and step sites are now visible. This suggests that the CO oxidized in the feature corresponding to CO oxidized at the (110) sites, is not necessarily adsorbed at the steps. It is more likely that CO adsorbed on the terrace *near* the step

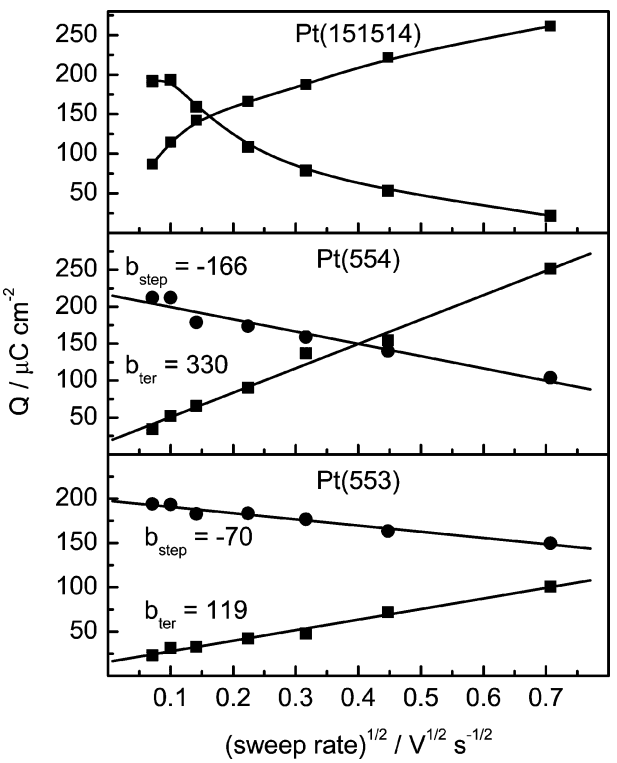

Fig. 10 Charge densities Q_{ter} (square) and Q_{step} (circle) *versus* the square root of the sweep rate for Pt(151514). Pt(554), Pt(553). Solid lines are the least-squares fits of the Pt(554) and Pt(553) data. The slopes "b" are in μC cm^{-2} V$^{-1/2}$ s$^{1/2}$.

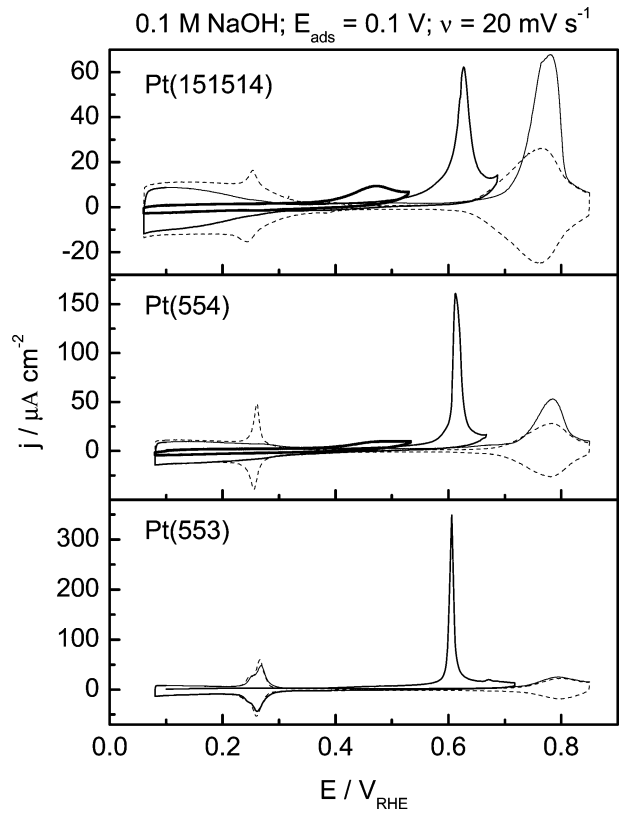

Fig. 11 CO stripping voltammetry observed by returning at different final potential: Scan reversed after kink-related CO oxidation (thick solid line), after step-related CO oxidation (thick dotted line), after terrace-related CO oxidation (thick double dot dashed line) and the subsequent cyclic voltammogram (thin dotted line) for Pt(15 15 14), Pt(554) and Pt(533) in 0.1 M NaOH, sweep rate 20 mV s^{-1}, E_{ads} = 0.1 V. For detailed explanation, see text.

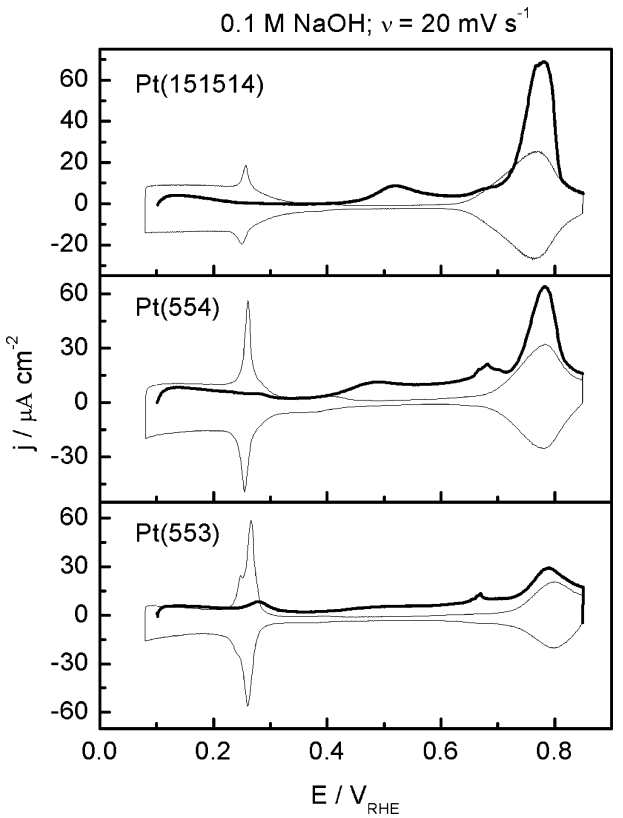

Fig. 12 CO stripping (thick solid line) after fast CO oxidation at step site at 500 mV s^{-1} (not shown) and subsequent cyclic voltammogram (thin solid line) for Pt(15 15 14), Pt(554) and Pt(533) in 0.1 M NaOH, sweep rate 20 mV s^{-1}, E_{ads} = 0.1 V. For detailed explanation, see text.

reacts with step bound OH, similar to what has been suggested previously for CO oxidation on stepped Pt in acidic media.[6,18] Still, it cannot be completely excluded that the step-bound CO reacts with step-bound OH in the feature at 0.6 V, after which the steps are quickly repopulated with CO from the nearby terrace at potentials below 0.6 V. Finally, in the final potential scan only the main peak corresponding to CO oxidation at the terrace is observed (dash-dotted lines). As expected from the previous scan through the hydrogen region of the Pt(553) electrode, very little CO was left on this electrode. This experiment again illustrates the low mobility of CO on the Pt(111) terraces in alkaline solution. Fig. 12 shows the results of similar experiments with Pt(15 15 14), Pt(554) and Pt(553), with the difference that in this case, we chose to strip off the step-related feature in a fast first scan at 500 mV s^{-1} up to 0.77 V for Pt(15 15 14) and 0.76 V for the other surfaces (not shown), and next to have a second stripping voltammogram at a much lower scan rate (20 mV s^{-1}) up to 0.85 V. In the second slow scan, we observe a partial recovery of the terrace sites in the hydrogen region, whereas the step sites again remain blocked by (presumably) adsorbed CO. In the subsequent slow CO stripping, we can clearly see stripping peaks at 0.52 and 0.49 V for Pt(15 15 14) and Pt(554), respectively, and a wave at about 0.49 V for Pt(553), corresponding to CO oxidation at kink sites. Additionally, we can observe peaks at 0.68 V for Pt(554) and Pt(553), related to CO oxidation at (100) sites. The peak corresponding to CO oxidation at the terrace sites is still visible but small. Remarkably, the CO oxidation at the kink sites is now dominant. Apparently, these sites are now easier to reach than under the conditions of Fig. 6–8. A possible explanation is that by oxidation of CO adsorbed near the (110) step sites in the previous fast CO stripping scan, mobility of CO *along* the step sites has been made possible. As a result, CO will prefer to oxidize at a defect in the step, *i.e.* a kink site.

Fig. 13 shows the Tafel plots for CO stripping on Pt(15 15 14), Pt(554) and Pt(553) as the peak potential *vs.* logarithm of the scan rate. Note that these plots are very different from the one obtained for Pt(111), Fig. 5. Since on the Pt(15 15 14) electrode the lowest-potential feature, that we tentatively ascribed to kink sites, clearly exhibits a peak rather than a wave, we can include this feature in the Tafel plot. On the Pt(554) and Pt(553) surface, the step-related stripping features have Tafel slopes of 92 and 75 mV dec^{-1}, respectively. The main peak has a very low Tafel slope on both surfaces, 36 and 39 mV dec^{-1}. The same features on Pt(15 15 14) have Tafel slopes of 83 and 53 mV dec^{-1}, whereas the lowest-potential feature exhibits a Tafel slope of 64 mV dec^{-1}. The exact interpretation of these Tafel slopes remains elusive, however, as the amount of CO oxidized in these features also depends on the scan rate, see Fig. 9 and 10, and therefore the

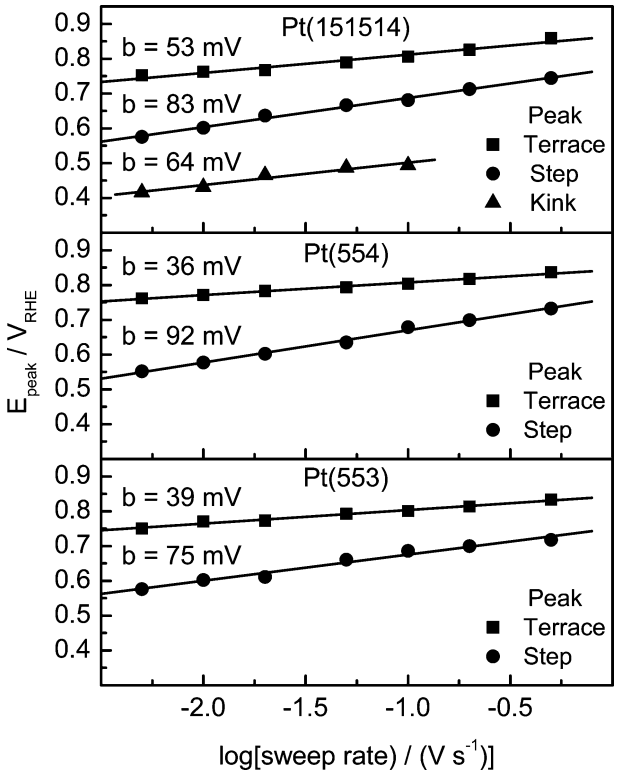

Fig. 13 Peak potential for CO oxidation *versus* the logarithm of the sweep rate for Pt(15 15 14), Pt(554) and Pt(533). Solid lines are the least-squares fits of the data.

peak potential does not only depend on the kinetics but also on the exact amount oxidized in each feature. Again, a detailed understanding requires kinetic modeling of the proposed surface processes.[19]

Pt(110)

Fig. 14 shows the CO stripping voltammetry from Pt(110) for various scan rates, and Fig. 15 gives the Tafel plot for the main peak, with a slope of 99 mV dec^{-1}. This slope agrees well with that observed (110)-step related CO stripping feature for the Pt(554) electrode, but is somewhat larger than the corresponding (110)-step related CO stripping feature for the Pt(553) electrode.

General discussion

From the results described in the previous sections, we conclude that CO oxidation on Pt single-crystal electrodes in alkaline solution may take place at four different active oxidation sites on the surface, the prominence of each oxidation reaction depending on the concentration of the corresponding site and time given to the terrace-bound CO to reach those sites. The least active site for CO oxidation, with the highest overpotential, is the terrace site, with an oxidation potential of *ca.* 0.7–0.8 V. Step sites of (110) and (100) orientation are more active than the terrace sites, with oxidation potentials at 0.6 and 0.68 V, respectively (at 20 mV s^{-1}). Finally, the most active sites have an oxidation potential as low as 0.35 V, and we tentatively ascribe these sites to low-coordination or kink sites on the surface. If given enough time

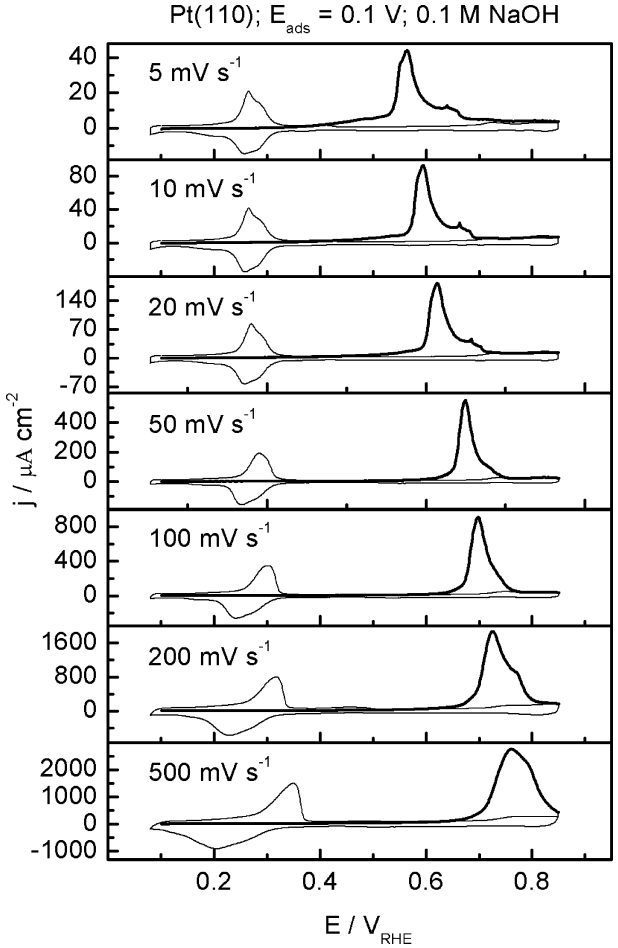

Fig. 14 CO stripping (thick solid line) and the subsequent cyclic voltammogram (thin solid line) for Pt(110) in 0.1 M NaOH at different sweep rates, E_{ads} = 0.1 V.

(*i.e.* at low scan rates), the voltammetric peak due to CO oxidized at terrace sites disappears and all terrace-bound CO will (slowly) diffuse to the more active sites and get oxidized there. In agreement with the conclusion drawn earlier by

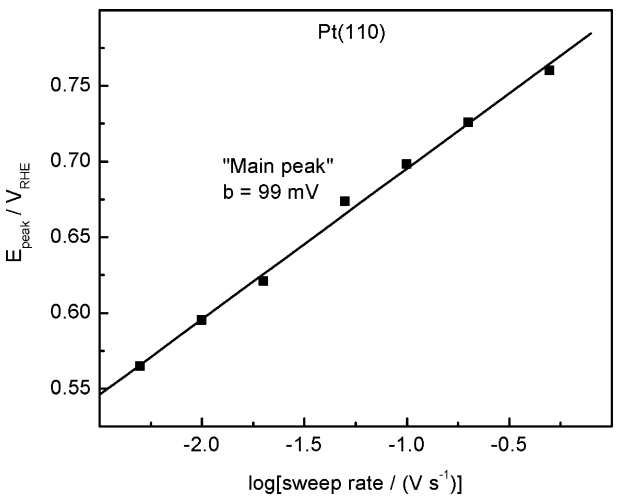

Fig. 15 Peak potential for CO oxidation *versus* the logarithm of the sweep rate for Pt(110). Solid lines is the least-squares fit of the data.

Spendelow *et al.*,[9] we believe that on all these sites, the CO oxidation follows a Langmuir–Hinshelwood mechanism, *i.e.* a reaction between CO_{ads} and OH_{ads}, on the basis of a peaked current transient observed in a constant-potential chronoamperometry experiment. We will discuss the chronoamperometry of the CO monolayer oxidation on stepped Pt electrodes in alkaline solution in more detail in a future publication.

The Tafel slopes obtained from these stripping experiments are somewhat difficult to interpret because the amount of CO oxidized at each site depends on the scan rate, and this in turn will influence the peak potential. Nevertheless, since this effect seems to be minimal on the Pt(111) electrode, and our Tafel slopes for that surface agree well with the slopes obtained by Spendelow *et al.*, we believe that a possibly meaningful interpretation may be the following. The Tafel slope for the main peak is 67 mV dec^{-1} in our experiment (73 mV dec^{-1} in Spendelow's experiments) and is very similar to previously published Tafel slopes for the oxidation of CO on stepped Pt electrodes, including Pt(111), in sulfuric acid electrolyte.[5] The most straightforward explanation for this Tafel slope is a rate-determining step between CO_{ads} and OH_{ads}:

$$H_2O + * \leftrightarrow OH_{ads} + H^+ + e^- \quad (3)$$

$$CO_{ads} + OH_{ads} \rightarrow COOH_{ads} \text{ (rate-determining step)} \quad (4)$$

$$COOH_{ads} \rightarrow CO_2 + H^+ + e^- + * \quad (5)$$

The Tafel slope observed in the prepeak region, 118 mV dec^{-1} in our experiments, and 130 mV dec^{-1} in Spendelow's experiments, was interpreted by Spendelow as reflecting repulsive lateral interactions in the CO/OH adlayer. An alternative explanation, we believe, could be the rate-determining formation of OH in the CO adlayer, *i.e.*

$$H_2O + * \rightarrow OH_{ads} + H^+ + e^- \quad (6)$$

followed by eqn 4 and 5. Although this reaction should be quite fast on a clean CO-free Pt surface, it may be inhibited by the presence of CO on the surface. At the present time, with the available data, it is not really possible to decide which explanation would be the most plausible. We do feel, however, that the explanation offered by Spendelow *et al.* is very sensitive to the actual values of the lateral interaction parameters (see their eqn (14)[9]), and it is rather coincidental that such a relatively complicated explanation leads to a Tafel slope that could be easily explained by a simpler mechanism not involving the assumption of lateral interactions.

The final two observations that remain to be understood relate to the role of the alkaline medium. First of all, why is CO oxidation faster in alkaline solution than in acidic solution, even on the pH-corrected RHE potential scale? Second, why is the apparent mobility of CO on the (111) terrace so low in alkaline solution, when we previously concluded that it is very high in acidic solution? Our tentative explanation for both effects involves electronic considerations, to be scrutinized by future spectroscopic measurements. Although the RHE scale corrects nicely for all pH dependent processes, such as hydrogen and OH adsorption, it overlooks all those adsorption processes that depend on the electrode potential but NOT on pH. One prominent example may be the actual adsorption strength of CO itself. The binding of CO at, say, 0.1 V *vs.* RHE in alkaline solution is different electronically from binding of CO at the same 0.1 V *vs.* RHE in acidic solution, because the electrode potential *vs.* the NHE is more negative and therefore the platinum Fermi level is more positive in alkaline solution than in acidic solution. This influences CO bonding, and evidence for this can be gleaned from the FTIR experiments by Markovic *et al.*[7] of CO adsorbed on Pt(111) in acidic and alkaline solution in the presence of CO in solution. In acidic solution, at 0.1 V *vs.* RHE, the CO spectrum shows bands centered at 2067 cm^{-1} and 1780 cm^{-1}, corresponding to atop and threefold hollow CO. In alkaline solution, at 0.1 V *vs.* RHE, the CO spectrum shows bands centered at 2036 cm^{-1} and 1733 cm^{-1}. These frequencies are significantly lower than in acidic solution, and reflect an increased back donation caused by a more negative electrode potential or more positive Pt Fermi level (with respect to the pH-independent levels in solution). To some extent, this effect is simply due to a Stark tuning. Since the pH difference between the two solutions is 12, corresponding to a potential shift of *ca.* 0.71 V, the corresponding Stark tuning slopes would be 40 and 60 cm^{-1} V^{-1} for the atop and threefold hollow CO. It is to be expected that this difference in binding to the surface must somehow be reflected in the kinetics of CO oxidation. Similarly, the binding energy of OH_{ads} may vary with potential, although Fig. 1 suggests that this effect is small for OH on the terraces.

Of the possible explanations for the reduced CO mobility in alkaline solution, we may consider the following two. First, the reduced CO mobility may be caused by a co-adsorbing species, as we have suggested for CO oxidation on Rh stepped single-crystals in sulfuric acid, where strongly adsorbed sulfate blocks CO mobility.[20] In alkaline solution, the only possible candidate for such a species would be the hydroxide OH^-. This would mean, however, that we would have to allow for OH^- *specific adsorption* on Pt(111) in the double-layer region, whereas the actual electrochemical reaction associated with the OH *chemisorption* to form OH_{ads} on the surface takes place only at potentials higher than 0.6 V *vs.* RHE. A second explanation is based on electronic arguments similar to those given in the previous paragraph. It is well known from previous FTIR experiments of CO adsorption on Pt(111) that with more negative potential there is an increasing propensity for CO to occupy threefold hollow sites as compared to atop sites.[21] This experimental observation was explained by density functional theory calculations,[22–24] which showed that at more negative potentials, the binding of CO to the threefold hollow site is favored over the atop site. According to the DFT calculations, the difference in binding energy is expected to become larger with more negative potential. The reason for this is that at more negative potential, or higher Pt Fermi level, there is an enhanced effect of back donation. Since back donation is a bonding interaction in terms of the Pt–CO bond, and bonding interactions typically favor multifold coordination, the threefold hollow site is expected to be the dominant binding site with more negative electrode potential. As a result, not only the binding energy *per se*, but also the binding energy differences between the different sites are expected to vary with potential. These binding energy differences between

various sites determine the activation energy for surface diffusion. Therefore, we may expect that at very negative potentials *vs*. NHE, such as in alkaline solution, larger binding energy differences exist between hollow, bridge and atop sites, and the CO surface diffusion will slow down accordingly. It is fair to note that the FTIR experiments by Markovic *et al*.[7] do not give direct evidence for this explanation, as the contribution from atop and threefold-hollow binding appears roughly the same from the spectra in alkaline and acidic solution (Fig. 2 and 4 in their paper). However, these experiments were carried out in the presence of CO in solution, which means that at low potentials *vs*. RHE, the CO adlayer is always saturated and the effects of lateral interactions and efficient packing may dominate over single-site binding energies. Clearly, dedicated FTIR experiments are needed to further study the role of CO binding in alkaline *vs*. acidic solution, and such experiments are currently planned in our laboratory.

4. Conclusions and summary

The electrochemical oxidation of a CO adlayer on Pt[n(111)×(111)] electrodes, with n = 30, 10, and 5, Pt(111), Pt(110) electrodes as well as a Pt(553) electrode (with steps of (100) orientation) in alkaline solution (0.1 M NaOH) has been studied employing stripping voltammetry. A minimal effect on electrode surface structure after CO oxidation has been observed for Pt(111) and the stepped electrodes, whereas a more pronounced change was observed for the Pt(110), due to the lower stability of the more open surface. On the surfaces studied, it is possible to distinguish CO oxidation at four different active oxidation sites on the surface, *i.e*. sites with (111), (110) and (100) orientation, and kink sites. This behavior is in strong contrast to CO stripping in acidic media. The least active site for CO oxidation is the (111) terrace site. The step sites are more active than the (111) terrace sites, the (110) site oxidizing CO at lower potential than the (100) site. The lowest potential CO oxidation feature (oxidation potential as low as 0.35 V *vs*. RHE) was ascribed to oxidation of CO at kink sites. The amount of CO oxidized at the active step or kink sites *vs*. the amount of CO oxidized at the (111) terrace sites depends on the concentration of the active sites and the time given to the terrace-bound CO to reach the active site. By performing CO stripping on the stepped surfaces at different scan rates, the diffusion of terrace-bound CO was clearly demonstrated, with most CO oxidized at the terrace at high scan rates, and most or all CO oxidized at the steps and kinks at low scan rate. The possible role of electronic effects in explaining the unusual activity and dynamics of CO adlayer oxidation in alkaline solution was discussed.

Acknowledgements

G. García is grateful to the Government of the Canary Islands for a research fellowship. The research program of M. T. M. Koper is supported by a VICI grant from the Netherlands Organization for Scientific Research (NWO).

References

1. N. M. Markovic and P. N. Ross, *Surf. Sci. Rep*., 2002, **45**, 117.
2. B. Love and J. Lipkowski, *ACS Symp. Ser*., 1988, **378**, 484.
3. H. Massong, S. Tillmann, T. Langkau, E. A. Abd El Meguid and H. Baltruschat, *Electrochim. Acta*, 1998, **44**, 1379.
4. N. P. Lebedeva, M. T. M. Koper, E. Herrero, J. M. Feliu and R. A. van Santen, *J. Electroanal. Chem*., 2000, **487**, 37.
5. N. P. Lebedeva, M. T. M. Koper, J. M. Feliu and R. A. van Santen, *J. Phys. Chem. B*, 2002, **106**, 12938.
6. M. T. M. Koper, N. P. Lebedeva and C. G. M. Hermse, *Faraday Discuss*., 2002, **121**, 301.
7. N. M. Markovic, C. A. Lucas, A. Rodes, V. Stamenkovic and P. N. Ross, *Surf. Sci*., 2002, **499**, L149.
8. J. S. Spendelow, G. Q. Lu, P. J. A. Kenis and A. Wieckowski, *J. Electroanal. Chem*., 2004, **568**, 215.
9. J. S. Spendelow, J. D. Goodpaster, P. J. A. Kenis and A. Wieckowski, *J. Phys. Chem. B*, 2006, **110**, 9545.
10. J. R. Varcoe and R. C. T. Slade, *Fuel Cells*, 2005, **5**, 187.
11. E. R. Choban, L. J. Markoski, A. Wieckowski and P. J. A. Kenis, *J. Power Sources*, 2004, **128**, 54.
12. J. S. Spendelow and A. Wieckowski, *Phys. Chem. Chem. Phys*., 2007, **9**, 2654.
13. J. Clavilier, D. Armand, S. G. Sun and M. Petit, *J. Electroanal. Chem*., 1986, **205**, 267.
14. N. S. Marinkovic, N. M. Markovic and R. R. Adzic, *J. Electroanal. Chem*., 1992, **330**, 433.
15. A. Lopez-Cudero, A. Cuesta and C. Guttierez, *J. Electroanal. Chem*., 2005, **579**, 1.
16. M. T. M. Koper, A. P. J. Jansen, R. A. van Santen, J. J. Lukkien and P. A. J. Hilbers, *J. Chem. Phys*., 1998, **109**, 6051.
17. A. J. Bard and L. R. Faulkner, *Electrochemical Methods, Fundamentals and Applications*, Wiley & Sons, New York, 2001.
18. N. P. Lebedeva, A. Rodes, J. M. Feliu, M. T. M. Koper and R. A. van Santen, *J. Phys. Chem. B*, 2002, **106**, 9863.
19. T. H. M. Housmans, C. G. M. Hermse and M. T. M. Koper, *J. Electroanal. Chem*., 2007, **607**, 67.
20. T. H. M. Housmans and M. T. M. Koper, *Electrochem. Commun*., 2005, **7**, 581.
21. I. Villegas and M. J. Weaver, *J. Chem. Phys*., 1994, **101**, 1684.
22. M. T. M. Koper and R. A. van Santen, *J. Electroanal. Chem*., 1999, **474**, 64.
23. M. T. M. Koper, R. A. van Santen, S. A. Wasileski and M. J. Weaver, *J. Chem. Phys*., 2000, **113**, 4392.
24. S. A. Wasileski, M. J. Weaver and M. T. M. Koper, *J. Electroanal. Chem*., 2001, **500**, 344.